# AJNR

**Calcified Intracranial Lesions: Detection with Gradient-Echo-Acquisition Rapid MR Imaging**

Scott W. Atlas, Robert I. Grossman, David B. Hackney, John M. Gomori, Nicholas Campagna, Herbert I. Goldberg, Larissa T. Bilaniuk and Robert A. Zimmerman

# Calcified Intracranial Lesions:
## Detection with Gradient-Echo-Acquisition Rapid MR Imaging

Scott W. Atlas[1, 2]
Robert I. Grossman[1]
David B. Hackney[1]
John M. Gomori[1]
Nicholas Campagna[3]
Herbert I. Goldberg[1]
Larissa T. Bilaniuk[1]
Robert A. Zimmerman[1]

Seventeen patients with partially calcified intracranial lesions, as documented by CT, were evaluated with MR imaging at 1.5 T. All patients were imaged with both conventional spin-echo techniques and reduced flip-angle gradient-echo-acquisition (GEA) sequences, during which a signal is acquired in the absence of a 180° radiofrequency pulse. GEA parameters were implemented so that T2* effects were maximized on these scans. In all 17 patients GEA images showed marked hypointensity throughout the entire area of calcification, matching the calcified region as seen on CT. In contrast, spin-echo findings in the calcified portions of the lesions were extremely variable, precluding confident identification of calcification on these images. The depiction of regions of calcification as marked hypointensity on GEA images can be ascribed to T2* shortening from static local magnetic field gradients at interfaces of regions differing in magnetic susceptibility, a phenomenon that is well documented in vitro, when various diamagnetic solids are placed in aqueous suspension. However, we cannot exclude the possible additional role of accompanying paramagnetic ions, which sometimes are present with diamagnetic calcium salts in various intracranial calcifications. Since the hypointensity due to calcification on GEA images is not specific, noncontrast CT could be used to confirm its presence.

Although this lack of specificity and the artifacts that emanate from diamagnetic susceptibility gradients at or near air–brain interfaces somewhat limit the application of GEA techniques, we suggest that rapid MR imaging using GEA sequences can consistently demonstrate intracranial calcification, and that this technique thus seems to be a useful adjunct to conventional spin-echo imaging.

Although spin-echo (SE) MR imaging has rapidly evolved into the most sensitive imaging technique for detection of most intracranial diseases [1, 2], one of its deficiencies lies in its well-recognized inability to detect calcification consistently [1–4]. Since the detection of calcification within certain intracranial lesions can provide important differential information, and because CT is highly sensitive for calcification, this has been regarded as a limitation of MR, both as a screening tool for certain diseases and as an aid to specific diagnosis.

Recently, investigators have used gradient-echo signal acquisition (GEA) rather than conventional SE techniques to maximize the detection of lesions having magnetic susceptibility differences, since T2* effects due to static field gradients created by these susceptibility differences are rephased by the 180° radiofrequency pulse used in SE sequences [5–9]. This technique has been especially useful in demonstrating previously undetectable signal intensity information from SE MR imaging at low to mid-field strengths [5, 8]. Furthermore, it is well documented in vitro that the introduction of various particulate solids into suspension creates abrupt magnetic susceptibility gradients that change static local magentic fields slightly, and consequently shorten T2* [10–14]. Early in our experience with reduced flip-angle GEA rapid MR imaging, we noted that calcified choroid plexus was consistently and markedly hypointense on GEA images, whereas these same areas were usually not delineated by SE images (Fig. 1). This observation prompted

A                                    B                                    C

Fig. 1.—Calcified choroid plexus in lateral ventricles. Note CT-documented calcifications in choroid plexus of lateral ventricles (*arrows* in *A*), although not discernible on long TR/TE spin-echo image (*B*), are markedly hypointense on gradient-echo-acquisition MR image (*arrows* in *C*).
*A*, Axial CT scan.
*B*, Axial spin-echo MR image (TR = 2500, TE = 80 msec).
*C*, Axial gradient-echo-acquisition MR image (TR = 750, TE = 50 msec, flip angle = 10°).

our study, in which we assessed the utility of in vivo GEA rapid MR imaging at 1.5 T for the detection of calcification within intracranial lesions.

## Subjects and Methods

Seventeen patients, ages 3–83 years, with CT-documented partially calcified intracranial lesions underwent MR imaging. All patients were studied with both conventional SE and GEA pulse sequences at 1.5 T on a General Electric Signa system. SE pulse sequences were used with both short repetition time (TR) (TR = 600 msec) and long TR (TR = 2500–3000 msec). Echo times (TE) ranged from 20–120 msec in these sequences. GEA sequences used TR of 200 (eight patients), 250 (one patient), or 750 (eight patients) msec, with TE of 50 msec and flip angle of 10° in all patients, so that contrast was based mainly on T2* differences [6]. GEA sequences used either sequentially acquired single-slice techniques with gradient-recalled acquisition in the steady state (GRASS) [15] or multisection acquisition partial saturation (PSI) [16] sequences. TR was limited to 250 msec in the sequential acquisition GRASS sequence to reduce total scan time, while a longer TR was used in the multisection acquisition PSI technique for purposes of improving signal/noise (without adding prohibitively to scan time).

Focal regions of calcification within all lesions were diagnosed on the basis of their appearance on CT. In all 17 cases, focal areas of calcification as documented by CT were compared with the appearance of these same regions on both SE and GEA MR images. All images were reviewed with both CT and MR studies present for comparison.

## Results

Calcified portions of the lesions were defined on the basis of their CT appearance. Sixteen of 17 lesions seen on CT were depicted by SE MR. The exception was an enhancing parietooccipital lobe with finely stippled calcification on CT in a patient with Sturge-Weber syndrome, whose SE MR demonstrated only malformed white matter but failed to show focal abnormal signal intensity. All 17 lesions were depicted clearly by GEA MR images.

In the 17 patients, SE images were extremely variable in their depiction of the calcified areas of the lesions. In 10 cases, the calcified regions were of variable or mixed signal intensity on SE sequences, not clearly separable from non-calcified portions of the lesion (Fig. 2). In two cases, parts of

the calcified areas were equally hypointense on all SE sequences, but only in a small portion of the CT-documented calcified region (Fig. 3). In four cases, equal hypointensity on all SE sequences was demonstrated throughout nearly the entire area of calcification (Fig. 4). In one case, high signal intensity was present in the area of calcification on all SE sequences (Fig. 5).

In all 17 cases, GEA images demonstrated marked hypointensity throughout the entire area of calcification as seen on CT (Figs. 2–5). This hypointensity closely matched the region of calcification demonstrated by CT. In all cases in which SE images demonstrated hypointensity in portions of the calcified areas, the hypointensity was more pronounced and/or more extensive on the GEA images.

## Discussion

The property of magnetic susceptibility of a material is determined by that material's magnetic response to an applied constant magnetic field. When placed in such a field, all tissues respond with an induced magnetic field of their own, the magnitude and direction of which vary among different tissues. Most human tissues are *diamagnetic*; that is, the induced field is weakly opposed to the applied magnetic field. *Paramagnetic* materials (e.g., hemosiderin, ferritin) respond with a magnetic field that weakly augments the applied field, while *ferromagnetic* materials respond with an induced field as strong as or stronger than the applied field, also in the same direction of that applied field [17].

The implementation of MR signal acquisition using gradient refocusing instead of the 180° pulse used in conventional SE sequences has enhanced the sensitivity of MR imaging for the detection of lesions having magnetic susceptibility variations, some of which were not easily detectable by SE MR imaging at low to mid-field strengths [5–9]. The success of this technique is based on the exploitation rather than the suppression of T2* effects, which are intentionally rephased by the 180° pulse in SE sequences [18, 19]. The signal loss occurring in GEA sequences that is not demonstrated by SE sequences can be attributed to variations in either static local magnetic susceptibilities or applied magnetic field ($B_o$) inhomogeneities. In the face of local magnetic field gradients, rapid dephasing of protons due to T2* decay occurs. This results

Fig. 2.—Calcified oligodendroglioma. Dense calcification on CT scan (*arrow* in *A*) in left frontal mass is mixed signal intensity on short TR/TE (*B*) and long TR/TE (*C*) spin-echo MR images, not clearly separable from noncalcified regions of lesion. MR image (*D*) demonstrates marked hypointensity throughout calcified portion of lesion (*arrow*), matching region of calcification on CT scan (*A*).
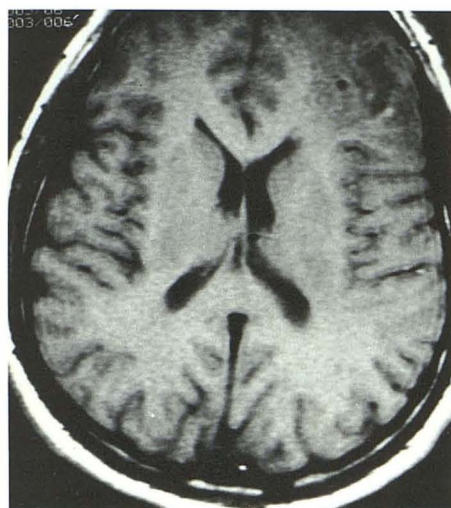
*A*, Axial CT scan.
*B*, Axial spin-echo MR image (TR = 600, TE = 20 msec).
*C*, Axial spin-echo MR image (TR = 2500, TE = 80 msec).
*D*, Axial gradient-echo-acquisition MR image (TR = 750, TE = 50 msec, flip angle = 10°).
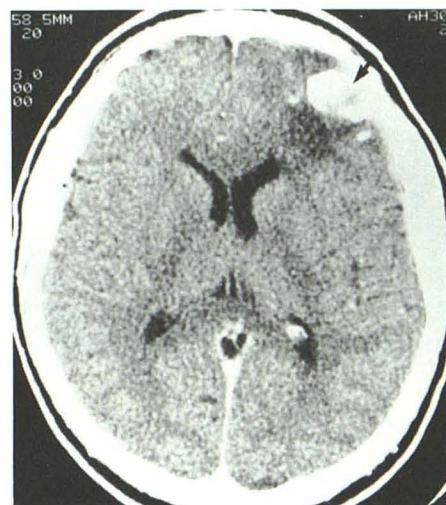


in signal loss when gradient reversal is used to generate the echo for signal acquisition. In contrast, the 180° pulse in the SE sequence recovers T2*-based signal decay [18, 19]; in fact, the SE pulse sequence was designed for that purpose. The sensitivity of gradient refocused pulse sequences for the detection of magnetic susceptibility effects (i.e., T2* effects) is increased by lengthening TE [5, 6]; T1 contrast dependence is reduced by decreasing the flip angle [6]; imaging time is shortened by reducing the TR [6]. Therefore, images that are highly dependent on T2* contrast can be acquired in a relatively short time by imaging with gradient refocusing using short TR, long TE, and short flip angle [6, 7, 15].

Many investigators have noted an alteration in local magnetic fields when various particulate solids are introduced into suspension in vitro [10–14]. The cause of this effect lies in the diamagnetic susceptibility gradients that occur at the interface of these solid particles and water protons. This produces local field gradients, which cause rapid proton precessional phase dispersal and consequent net intravoxel

phase cancellation (i.e., T2* shortening) and, therefore, signal loss. Similar mechanisms are responsible for signal drop-off at or near air–brain (i.e., paranasal sinus–brain) interfaces (Fig. 6) and at the boundaries of intraparenchymal hemorrhage [5, 7, 9, 15]. This mechanism of intravoxel proton dephasing is distinctly different from true T2 shortening from varying local field inhomogeneities experienced by diffusing water protons during the interecho time of a 180° pulse SE experiment, which varies as the square of the applied magnetic field [20, 21] and cannot be reversed by the 180° pulse. T2* effects are linearly related to the applied magnetic field, and therefore magnetic susceptibility effects would theoretically be more prominent at higher applied field strengths [5].

In our series, focal calcifications within intracerebral lesions were consistently displayed as focal areas of markedly low signal intensity on GEA scans. In contrast, as has been repeatedly documented in the literature [3, 4], SE signal intensity patterns were extremely variable in these same areas, so that no reliable documentation of calcification was
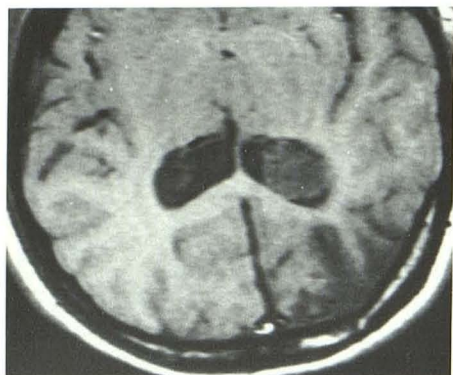
A

Fig. 3.—Parietooccipital calcification in Sturge-Weber syndrome. Extensive calcification in left posterior parietooccipital lobe on CT scan (A) is hypointense, but only in a small portion of calcified region, on both short TR/TE (B) and long TR/TE (C) spin-echo MR images. Gradient-echo-acquisition MR image (D) demonstrates marked hypointensity throughout entire area of calcification, again matching CT-documented calcified region (A).

A, Axial CT scan.
B, Axial spin-echo MR image (TR = 600, TE = 20 msec).
C, Axial spin-echo MR image (TR = 2500, TE = 80 msec).
D, Axial gradient-echo-acquisition MR image (TR = 750, TE = 50 msec, flip angle = 10°).



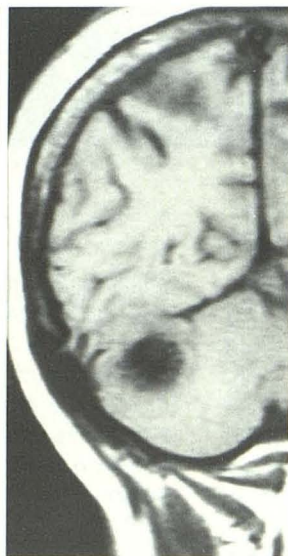B                                    C                                    D
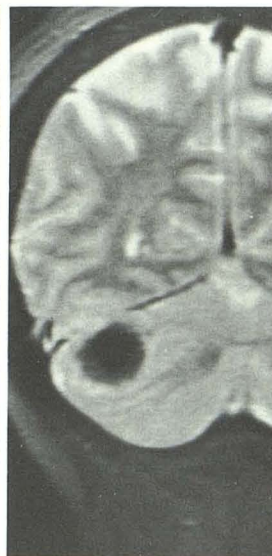


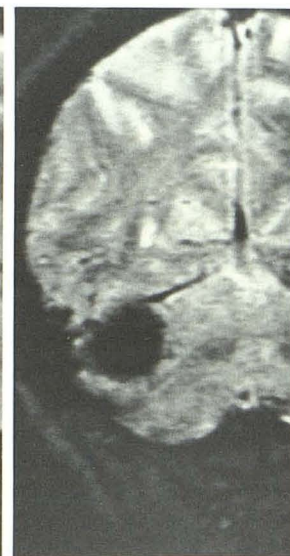A                                    B                                    C                                    D

Fig. 4.—Densely calcified posterior fossa meningioma. Densely calcified meningioma in right posterior fossa on CT scan (arrow in A) is hypointense throughout most of the area of calcification on both short TR/TE (B) and long TR/TE (C) spin-echo MR images. Note that hypointensity is more profound and extensive on gradient-echo-acquisition MR image (D), due to both an increased sensitivity to the more peripheral aspects of the calcified mass and possibly to a "blooming" effect from magnetic susceptibility differences between the lesion and adjacent brain.

A, Axial CT scan.
B, Coronal spin-echo MR image (TR = 600, TE = 20 msec).
C, Coronal spin-echo MR image (TR = 2500, TE = 80 msec).
D, Coronal gradient-echo-acquisition MR image (TR = 750, TE = 50 msec, flip angle = 10°).

Fig. 5.—Densely calcified corpus callosum glioma. Dense calcification throughout tumor involving genu of corpus callosum on CT scan (*A*) is high intensity on both short TR/TE (*B*) and long TR/TE (*C*) spin-echo MR images. Note marked hypointensity throughout entire calcified region of lesion on gradient-echo-acquisition MR image (*D*).
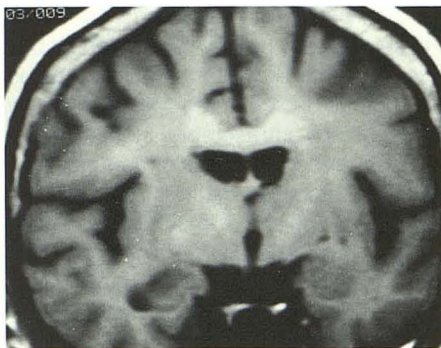
    *A*, Axial CT scan.
    *B*, Coronal spin-echo MR image (TR = 600, TE = 20 msec).
    *C*, Coronal spin-echo MR image (TR = 2500, TE = 80 msec).
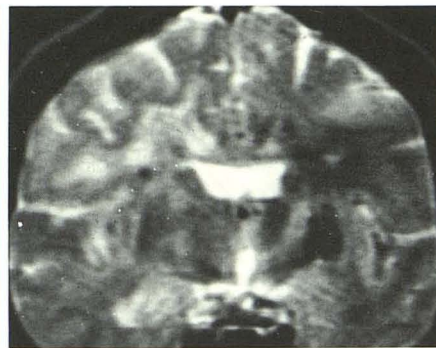    *D*, Coronal gradient-echo-acquisition MR image (TR = 750, TE = 50 msec, flip angle = 10°).
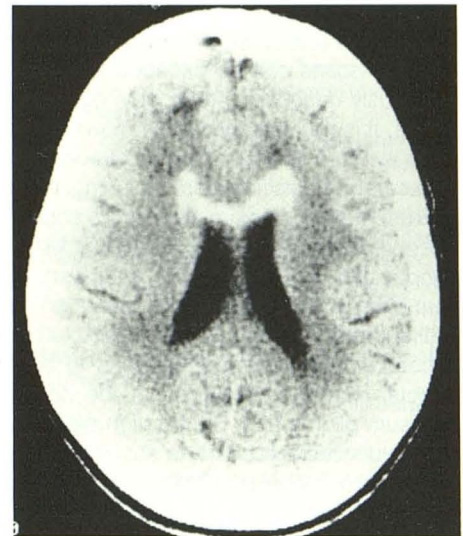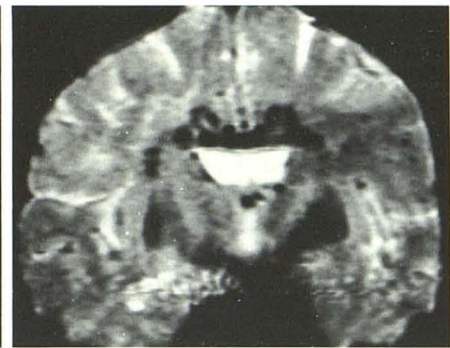


A



B



C



D

Fig. 6.—Diamagnetic susceptibility artifacts on T2*-weighted gradient-echo-acquisition MR images. Note extensive hypointensity obscuring inferior temporal lobes and subfrontal region, due to diamagnetic susceptibility differences at air–brain interfaces (between paranasal sinuses or mastoid air cells and adjacent brain parenchyma).

    *A*, Axial gradient-echo-acquisition MR image (TR = 750, TE = 50 msec, flip angle = 10°), inferiorly.

    *B*, Axial gradient-echo-acquisition MR image (TR = 750, TE = 50 msec, flip angle = 10°), more superiorly.



A



B

possible with this sequence. Furthermore, in the cases in which SE imaging displayed a part of the calcified portion of the lesion as low intensity, the GEA image demonstrated more extensive and/or more profound hypointensity in all but one case. This trend was also noted in calcified choroid plexuses, where GEA images consistently demonstrated marked hypointensity, whereas SE sequences usually did not detect any signal intensity difference correlating to the pres-

ence of CT-documented calcification (Fig. 1). The depiction of calcification (a diamagnetic material) as marked hypointensity on GEA scans can be ascribed to T2* shortening from the previously described static local magnetic susceptibility gradients. It is not entirely certain, however, that the calcification itself in the true cause of the hypointensity in these cases. Intracerebral calcifications, including those found in choroid plexus, meningiomas, pineal gland, and Fahr disease have all been variably noted to be accompanied by the deposition of various cationic species (e.g., zinc, iron, copper, manganese, aluminum) [22–25]. Therefore, although calcification is clearly present in our cases, we cannot exclude the possible role of accompanying paramagnetic ions in the production of T2* effects. In fact, in the case of the densely calcified corpus callosum glioma (Fig. 5), the high signal intensity seen on all SE sequences leads one to suspect that accompanying paramagnetic material is probably present in that case, in addition to the biopsy-proved calcium salts. More significantly, though, regardless of whether the calcium or other concomitantly deposited species are the actual cause of the consistent hypointensity on GEA MR images, we can now suggest the presence of calcification in these lesions without prior CT.

The GEA MR appearance of calcification is not specific. Aside from calcification, GEA images demonstrate this same marked hypointensity at the boundaries of or in the substance of various stages of intracerebral hemorrhage (i.e., deoxyhemoglobin, methemoglobin, hemosiderin) [5] and at the borders of melanotic lesions [26]. This boundary effect [5] occurs at any interface of regions differing in magnetic susceptibility, including paramagnetic, diamagnetic, and ferro-magnetic substances. As previously mentioned, the SE technique eliminates the detectability of such static locally inhomogeneous magnetic fields by virtue of the 180° rephasing pulse [18, 19]. SE images, on the other hand, depict intracellular paramagnetic species (such as deoxyhemoglobin or hemosiderin) as marked hypointensity on long TR/long TE sequences (preferential T2 shortening) [21]. This effect increases with many factors, including interecho time, the square of the applied magnetic field, and the concentration of the paramagnetic substance [21]. Dramatically increased hypointensity is therefore noted in these instances as one increases these factors [21], and it can be seen by comparing long TR/long TE SE images with long TR/short TE and short TR/short TE SE images. Densely calcified lesions that are depicted as hypointensity by SE images differ from these blood-breakdown products in that these calcifications are *equally* hypointense on all SE sequences; that is, there is no detectable preferential T2 shortening at field strengths up to 1.5 T. The lack of mobile protons in calcified regions has been proposed as the probable mechanism of this signal loss on SE images [2–4]. Therefore, it appears that the marked hypointensity preferentially seen on long TR/long TE SE images at 1.5 T is more specific than the marked hypointensity seen on GEA images. Furthermore, marked artifacts that obscure the inferior temporal lobes and subfrontal regions because of diamagnetic susceptibility gradients at or near air–brain interfaces preclude the use of this technique in its current form as a general screening method for detecting intracranial calcifi-

cation. We suggest that the role of GEA MR imaging for the detection of intracranial calcification be that of an adjunct to conventional SE imaging.

In summary, calcification within intracranial lesions, although variable in appearance and unreliably detected by SE techniques, can be consistently demonstrated by GEA rapid MR imaging using short TR, long TE, and short flip angles. Calcified regions were markedly hypointense in areas that matched CT-depicted calcified portions of these lesions in 17/17 patients. In cases in which SE images demonstrated hypointensity in portions of the calcified area of the lesion, the hypointensity was more marked and/or more extensive on the GEA image. The hypointensity on the GEA image matching the calcified part of the lesion is presumably a reflection of T2* shortening by static local magnetic field gradients created by the presence of diamagnetic calcium crystal deposits, effects that are intentionally rephased by the 180° pulse of the SE sequence. We cannot exclude the possible role of potentially accompanying cations, which have been variably found by other investigators in the presence of many intracranial calcifications. The dramatic hypointensity on the GEA images is nonspecific, however, and can also be seen in the presence of intracellular paramagnetic blood-breakdown products, such as deoxyhemoglobin or hemosiderin, at the boundaries of any intracerebral hematoma, in physiologic iron-containing areas of the brain, and indeed at the interface of any regions differing in magnetic susceptibility (e.g., melanin, air, blood, etc.). Chemical shift and some flow-related artifacts are also hypointense on GEA images. Noncontrast CT could therefore be used to confirm the presence of calcification in these cases. Furthermore, significant hypointensity arising from diamagnetic susceptibility gradients at or near air–brain interfaces limit the application of this technique at present to an adjunct to conventional SE imaging rather than as a general screening tool.

## REFERENCES

1. Brandt-Zawadzki M, Badami JP, Mills CM, Norman D, Newton TH. Primary intracranial tumor imaging: a comparison of magnetic resonance and CT. *Radiology* **1984**;150:435–440
2. Bradley WG Jr, Waluch V, Yadley RA, Wycoff RR. Comparison of CT and MR in 400 patients with suspected disease of the brain and cervical spinal cord. *Radiology* **1984**;152:695–702
3. Holland BA, Kucharcyzk W, Brandt-Zawadzki M, Norman D, Haas DK, Harper PS. MR imaging of calcified intracranial lesions. *Radiology* **1985**;157:353–356
4. Oot R, New PFJ, Pile-Spellman J, Rosen BR, Shoukimas GM, Davis KR. The detection of intracranial calcifications by MR. *AJNR* **1986**;7:801–809
5. Edelman RR, Johnson K, Buxton R, et al. MR of hemorrhage: a new approach. *AJNR* **1986**;7:751–756
6. Buxton RB, Edelman RR, Rosen BR, Wismer GL, Brady TJ. Contrast in rapid MR imaging: T1- and T2-weighted imaging. *J Comput Assist Tomogr* **1987**;11:7–16
7. Young IF, Khenia S, Thomas DGT, et al. Clinical magnetic susceptibility mapping of the brain. *J Comput Assist Tomogr* **1987**;11:2–6
8. Bydder GM, Payne JA, Collins AG, et al. Clinical use of rapid T2-weighted partial saturation sequences in MR imaging. *J Comput Assist Tomogr* **1987**;11:17–23
9. Cox IJ, Bydder GM, Gadian DG, et al. The effect of magnetic susceptibility variations in NMR and NMR spectroscopy *in vivo*. *J Mag Reson*

      **1986**;70:163–168

10. Glasel JA, Lee KH. On the interpretation of water nuclear magnetic resonance relaxation times in heterogeneous systems. *J Am Chem Soc* **1974**;96:970–978

11. Fung BM, McGaughy TW. Magnetic-relaxation in heterogeneous systems. *J Mag Reson* **1981**;43:316–323

12. Hanus F, Gillis P. Relaxation of water adsorbed on the surface of silica powder. *J Mag Reson* **1984**;59:437–445

13. Davis CA, Genant HK, Dunham JS. The effects of bone on proton NMR relaxation times of surrounding liquids. *Invest Radiol* **1986**;21:472–477

14. Packer KJ. The effects of diffusion through locally inhomogeneous magnetic fields on transverse nuclear spin relaxation in heterogeneous systems. Proton tranverse relaxation in striated muscle tissue. *J Mag Reson* **1973**;9:438–443

15. Wehrli F, Prost JH, Roberts F. The distinguishing properties of gradient-recalled acquisition in the steady state (GRASS). *Mag Reson Imag* **1987**;5(Suppl 1):105

16. Campagna N (personal communication), General Electric, Milwaukee, WI, **1987**

17. Brittenham GM, Farrell DE, Harris JW, et al. Magnetic-susceptibility measurement of human iron stores. *N Engl J Med* **1982**;307:1671–1675

18. Hahn EL. Spin echoes. *Phys Rev* **1950**;80:580–594

19. Carr HY, Purcell EM. Effects of diffusion on free precession in nuclear magnetic resonance experiments. *Phys Rev* **1954**;94:630–638

20. Thulborn KR, Waterton JC, Matthews PM, Radda GK. Oxygen dependence of the transverse relaxation time of water protons in whole blood at high field. *Biochim Biophys Acta* **1982**;714:265–270

21. Gomori JM, Grossman RI, Goldberg HI, Zimmerman RA, Bilaniuk LT. Intracranial hematomas: imaging by high-field MR. *Radiology* **1985**;157:87–93

22. Duckett S, Galle P, Escourolle R, Poirier J, Hauw J. Presence of zinc, aluminum, magnesium in Striopalledodentate (SPD) calcification (Fahr's disease): electron probe study. *Acta Neuropathol (Berl)* **1977**;38:7–10

23. Alcolada JC, Moore IE, Weller RO. Calcification in the human choroid plexus, meningiomas and pineal gland. *Neuropathol Appl Neurobiol* **1986**;12:235–250

24. Kozik M, Kulczycki L. Laser-spectroscopic analysis of the cation content in Fahr's syndrome. *Arch Psych Nerv* **1978**;225:135–142

25. Scotti G, Scialfa G, Tampieri D, Landoni L. MR imaging in Fahr disease. *J Comput Assist Tomogr* **1985**;9:790–792

26. Atlas SW, Grossman RI, Guerry D, et al. The detection of intracranial malignant melanoma metastases: increased sensitivity of gradient echo acquisition MR imaging. Poster presented at the annual meeting of the Society of Magnetic Resonance in Medicine, New York, August **1987**